REPORT DOCUMENTATION PAGE

AFRL-SR-BL-TR-01-

0443

1. REPORT DATE (DD-MM-YYYY)	2. REPORT TYPE	3. DATES COVERED (From - To)
19-06-2001	Final	April-November 2000

4. TITLE AND SUBTITLE
Application of Large Eddy Simulation to Cooling and Flow Problems in Aeropropulsion Systems

5a. CONTRACT NUMBER

5b. GRANT NUMBER
AFOSR F49620-00-1-0229

5c. PROGRAM ELEMENT NUMBER

6. AUTHOR(S)
Pletcher, R. H.

5d. PROJECT NUMBER

5e. TASK NUMBER

5f. WORK UNIT NUMBER

7. PERFORMING ORGANIZATION NAME(S) AND ADDRESS(ES)
Department of Mechanical Engineering
Black Engineering Building
Iowa State University
Ames, Iowa 50011

8. PERFORMING ORGANIZATION REPORT NUMBER
ISU-ERI-Ames-01619

9. SPONSORING / MONITORING AGENCY NAME(S) AND ADDRESS(ES)
Air Force Office of Scientific
Scientific Research/NA
Turbulence and Internal Flows
801 N. Randolph St.
Arlington, VA 22203-1977

10. SPONSOR/MONITOR'S ACRONYM(S)
AFOSR

11. SPONSOR/MONITOR'S REPORT NUMBER(S)

12. DISTRIBUTION / AVAILABILITY STATEMENT
Approved for public release; distribution unlimited

13. SUPPLEMENTARY NOTES

14. ABSTRACT
The objective of this research was to expand the capabilities of large eddy simulation technology to contribute to the solution of urgent problems in propulsion systems and to contribute to the physical understanding of such flows. Work was initiated on both external and internal cooling flows in turbines. Results on the effects of rotation on heat transfer in channel flow are reported for heating and cooling rates of magnitudes large enough to cause significant variation in temperature dependent fluid properties. The effect of rotation was to reduce the turbulent transport near the leading wall and increase it near the trailing wall. The effect was larger for the heating flows than for the cooling flow. The ratio of Nusselt numbers on the two walls ranged between two and five, whereas the friction coefficients at the trailing wall were about twice as large as those at the leading wall. The magnitudes of streamwise and spanwise velocity fluctuations were observed to differ by about a factor of two near the two walls.

15. SUBJECT TERMS
Large eddy simulation, turbulent flow, heat transfer

16. SECURITY CLASSIFICATION OF:			17. LIMITATION OF ABSTRACT	18. NUMBER OF PAGES	19a. NAME OF RESPONSIBLE PERSON
a. REPORT	b. ABSTRACT	c. THIS PAGE			19b. TELEPHONE NUMBER (include area code)
Unclassified	Unclassified	Unclassified	UU	i-iii 1-18 21 total	

Final Technical Report
AFOSR Grant F49620-00-1-0229

Report ISU-ERI-Ames-01619

APPLICATION OF LARGE EDDY SIMULATION TO COOLING AND FLOW PROBLEMS IN AEROPROPULSION SYSTEMS

Richard H. Pletcher
Department of Mechanical Engineering
and Computational Fluid Dynamics Center
Iowa State University
Ames, Iowa 50011

June 19, 2001

College of Engineering
Iowa State University

TABLE OF CONTENTS

1.0 INTRODUCTION

This report summarizes the research accomplishments achieved under Grant AFOSR F49620-00-1-0229, "Application of Large Eddy Simulation to Cooling and Flow Problems in Aeropropulsion Systems." The objective of the research was to expand the capabilities of LES technology to contribute to the solution of urgent problems in propulsion systems and to contribute to the physical understanding of such flows. The long-term goal of the thrust is to advance large eddy simulation (LES) technology to the point where it is effective for computing realistic flows in a rotating, multistage turbomachine. First, however, some building block simulations need to be carried out for a single blade element. The first task in the long-term research was to address cooling flows in turbines, both the film cooling of external blade surfaces and the complex flows in internal passages.

The grant duration was a short eight months so the scope of the work that could be completed in that period was very limited. Work was initiated on the external film cooling problem and some interesting results were obtained from a study on the effect of rotation on heat transfer in channel flow. The rotating channel flow heat transfer results represent one step toward the realistic simulation of internal cooling flows for turbine components. Rotation exerts an important influence on flows in turbomachines and needs to be taken into account in the design process. The remainder of this report will describe results obtained from the rotating channel study.

System rotation influences turbulence in several ways: for example, it may decrease energy transfer from large to small scales or reduce turbulence dissipation and decay rate of turbulence energy. In rotating channel flow, system rotation can both stabilize and

destabilize the flow. On the unstable side, Coriolis forces enhance turbulence production and increase the intensity of turbulence, while on the stable side, Coriolis forces reduce turbulence production and decrease the intensity of turbulence. Most large eddy simulations (LES) of flows with heat transfer reported to date employed an incompressible formulation and treated temperature as a passive scalar. However, compressible formulations have been employed in a few recent works (Moin et al. (1991), Nicoud (1998), Wang and Pletcher (1995; 1996), Dailey and Pletcher (1996; 1997; 1998), and Meng et al. (1999a; 1999b)) where the coupling between velocity and temperature fields were considered.

Many rotational-induced flow phenomena have been reported on by Tritton (1978; 1985) and Hopfinger, (1989). Rotating channel flows have been investigated experimentally (Johnston et al., 1972; Han et al., 1994) and numerically (Kristofferson and Andersson, 1993; Tafti, 1991) (by direct and large-eddy simulations). However, very little information is available for rotating channel flow with heat transfer, especially from the LES or DNS community. The goal of this facet of the research was to demonstrate and analyze the effects of system rotation on heat transfer in turbulent channel flow.

2.0 GOVERNING EQUATIONS

The governing equations for large eddy simulation were obtained by filtering the unsteady three-dimensional compressible Navier-Stokes equations. The filter, which separates the effects of the large-scale and small-scale motions, can be written in terms of a convolution integral as

$$\bar{f}(\vec{x},t) = \int_D G(\vec{x}-\vec{\xi}) f(\vec{x},t) d\vec{\xi} \qquad (1)$$

where G is some spatial filter with a width on the order of the grid spacing, and D is the flow domain. For compressible flows, the Favre-averaged filter is introduced which can be defined by

$$\tilde{f} = \frac{\overline{\rho f}}{\overline{\rho}} \tag{2}$$

The resulting equations were nondimensionalized with respect to a reference length δ, velocity V_r, density ρ_r, and viscosity μ_r. For the simulations in this report, δ is the half height of the channel, and V_r is the bulk velocity at the inlet. The resulting Favre-filtered nondimensional compressible forms of equations for conservation of mass, momentum are given below :

$$\frac{\partial \overline{\rho}}{\partial t} + \frac{\partial \left(\overline{\rho}\tilde{u}_j\right)}{\partial x_j} = 0 \tag{3}$$

$$\frac{\partial \left(\overline{\rho}\tilde{u}_i\right)}{\partial t} + \frac{\partial \left(\overline{\rho}\tilde{u}_i\tilde{u}_j\right)}{\partial x_j} = -\frac{\partial \overline{p}}{\partial x_i} + \frac{\partial \tilde{\sigma}_{ij}}{\partial x_j} - \frac{\partial \tau_{ij}}{\partial x_j} + 2\overline{\rho}\varepsilon_{ij3}\Omega\tilde{u}_j \tag{4}$$

$$\frac{\partial}{\partial t}(\overline{\rho}\tilde{E}) + \frac{\partial}{\partial x_j}\left[\overline{\rho}\tilde{E} + \overline{p})\tilde{u}_j\right] = -\frac{\partial \left(\tilde{u}_i\tilde{\sigma}_{ij}\right)}{\partial x_j} - \frac{\partial \overline{q}_j}{\partial x_j} - \frac{\partial q_{ij}}{\partial x_j} - \alpha - \pi - \varepsilon \tag{5}$$

In the equations above, $2\overline{\rho}\varepsilon_{ij3}\Omega\tilde{u}_j$ represents the Coriolis force, ε_{ij3} is Levi-Civita's alternating tensor and Ω is the angular velocity of the system. A traditional right-handed coordinate system is employed and the axis of rotation is in the positive z or x_3 direction. The resolved total energy is $\tilde{E} = c_v\tilde{T} + \frac{1}{2}\tilde{u}_i\tilde{u}_i$, the viscous stress tensor is

$$\tilde{\sigma}_{ij} = \frac{2\mu}{\mathrm{Re}_L}\left(\tilde{S}_{ij} - \frac{1}{3}\tilde{S}_{kk}\delta_{ij}\right) \tag{6}$$

where δ_{ij} is the Kronecker delta and the strain rate tensor and heat flux vectors are

$$\tilde{S}_{ij} = \frac{1}{2}\left(\frac{\partial \tilde{u}_i}{\partial x_j} + \frac{\partial \tilde{u}_j}{\partial x_i}\right) \tag{7}$$

$$q_j = -\frac{c_p \mu}{\mathrm{Re}_L \,\mathrm{Pr}} \frac{\partial \tilde{T}}{\partial x_j} \tag{8}$$

The Favre filtered equation of state is $\overline{p} = \overline{\rho} R \tilde{T}$. The viscosity and thermal conductivity were evaluated by using the power law variation with temperature.

$$\frac{\mu}{\mu_0} = \left(\frac{T}{T_0}\right)^{0.7}, \quad \frac{k}{k_0} = \left(\frac{T}{T_0}\right)^{0.7} \tag{9}$$

The Prandtl number was assumed to be constant at a value of 0.71.

The effects of the small scales are present in the above equations through the SGS stress tensor in the filtered momentum equation

$$\tau_{ij} = \overline{\rho}\left(\widetilde{u_i u_j} - \tilde{u}_i \tilde{u}_j\right) \tag{10}$$

The SGS heat flux and other quantities in the filtered energy equation are given by

$$q_{ij} = \overline{\rho} c_v \left(\widetilde{T u_j} - \tilde{T}\tilde{u}_j\right) \tag{11}$$

$$\alpha = u_i \frac{\partial\left(\overline{\rho}\tau_{ij}\right)}{\partial x_j} \tag{12}$$

$$\pi = \overline{p \frac{\partial u_i}{\partial x_i}} - \overline{p} \frac{\partial \tilde{u}_i}{\partial x_i} \tag{13}$$

$$\varepsilon = \overline{\sigma_{ij} \frac{\partial u_j}{\partial x_j}} - \tilde{\sigma}_{ij} \frac{\partial \tilde{u}_i}{\partial x_j} \tag{14}$$

For this research, the first three terms on the right-hand side of the energy equations were computed, but the remaining terms (α, π, ε) were neglected due to their relative smaller magnitudes.

3.0 NUMERICAL METHOD

In the present research, a compressible finite volume formulation (Dailey, 1997; Dailey and Pletcher, 1998; Meng et al., 1999b) was used to solve the governing equations, which also permits the subgrid-scale turbulent Prandtl number to be computed dynamically. The code used Cartesian hexahedral control volumes, and solved for the primitive variables (p, u, v, w, T) that were stored at the cell centers. Besides the physical time integration, pseudo time iterations were performed to resolve nonlinearities in the algebraic formulation and to implement the low Mach number preconditioning using an implicit LU-SGS scheme. The low Mach number preconditioning was used to enable the compressible code to work efficiently at nearly incompressible speeds. The solver is second-order accurate in both space and time (Dailey and Pletcher, 1996; Dailey 1997). The multiblock code was parallelized using the message passing interface (MPI). The computations were carried out on an IBM SP2 (Minnesota Supercomputing Institute) using 17 processors.

The simulations were run with a domain size of $2\pi \times 2 \times \pi$ with a grid that had $48 \times 64 \times 48$ control volumes in the x, y, and z directions, respectively. A grid study (Dailey, 1997) has shown that for low heating simulations without rotation, this grid size provided accurate results compared to DNS and experimental data. The near wall region was well-resolved. For the high heating case, the y^+ (based on averaged friction velocity) at the first grid point near the wall was less than 0.5, so no wall function was used.

When property variations are taken into account, flows with heating or cooling do not attain a fully developed state. However, experiments show that far downstream of the entry region, a slowly evolving quasi-developed state exists. Dailey (1997) and Dailey and Pletcher (1998) showed that for laminar flow with uniform heat flux conditions, use of step periodic boundary conditions can match the flow conditions that evolve from variable property developing flow. Inspection of a developing flow solution revealed that the following conditions held approximately in the downstream region:

$$\frac{\partial(\rho u)}{\partial x} = 0$$
$$\frac{\partial v}{\partial x} = 0$$
$$\frac{\partial w}{\partial x} = 0$$
$$\frac{\partial p}{\partial x} = constant$$
$$\frac{\partial T}{\partial x} = constant$$

Thus, Dailey (1997) concluded that a short section of the downstream region could be computed in a "stepwise periodic" manner with the following streamwise boundary conditions.

$$\rho u(0,y) = \rho u(L_x,y)$$
$$v(0,y) = v(L_x,y)$$
$$w(0,y) = w(L_x,y)$$
$$p_p(0,y) = p_p(L_x,y)$$
$$T(0,y) = T(L_x,y) - \Delta T_x$$

where L_x is the length of the computation domain in the streamwise direction and $\overline{p}_p$ is the periodic component of the pressure $\overline{p}(x,y,z,t) = \beta x + \overline{p}_p(x,y,z,t)$ where β is the average streamwise pressure gradient. The temperature difference ΔT is computed from

an energy balance utilizing the uniform heat flux imposed and the mass flux. All primitive variables were assumed to be periodic in the spanwise (z) direction.

No-slip velocity and zero normal pressure gradient boundary conditions were enforced at the upper and lower walls. The isoflux thermal wall boundary conditions were used for both walls. The dimensionless wall heat flux, $q_w = \frac{q_w^*}{c_p \rho_{ref} U_{ref} T_{ref}}$, was kept at 2×10^{-4} for the low heating case, and kept at 2×10^{-3} and -2×10^{-3} for the high heating and high cooling cases, respectively.

3.1 Dynamic Subgrid-Scale Stress Model

The compressible formulation for the dynamic model first proposed by Moin et al. (1991) was utilized in this research. The dynamic subgrid stress model uses information from two different grid levels to determine the coefficient in the Smagorinsky stress model dynamically. The dynamic model does not require ad hoc damping near solid walls and enables the turbulent Prandtl number to also be computed dynamically.

The dynamic model coefficient and the turbulent Prandtl number were averaged along the only homogeneous (spanwise) direction. Further details can be found in Meng and Pletcher (2000).

4.0 RESULTS

Caculations were performed for four different cases: no heat transfer, low heating, high heating, and high cooling. The Reynold number $\mathrm{Re} = V_r 2\delta / \nu$ (based on the channel width, 2δ, and reference velocity, V_r) was 5600, and the rotation number $Ro_b = |\Omega| 2\delta / V_r$ was 0.144. It should be noted that the results to be presented here are for a channel with

negative ($\Omega < 0$) angular velocity about the positive z-axis. The configuration can be seen in Fig. 1.

It should be noted that the results to follow are for channel flow rather than duct flow so no mean secondary flow is present. Such conditions represent the flow in the central part of a duct of large (in the limit, infinite) aspect ratio. The results from first case were compared with the DNS results (grid $96 \times 97 \times 128$) of Piomelli and Liu (1995) for the isothermal rotating channel flow with $\mathrm{Re}_b = U_b 2\delta / \nu = 5700$ and $Ro_b = 0.144$. Since it was found from previous LES simulations that the contribution of the SGS model to the turbulent flux is small, it was of interest to do a simulation (coarse grid DNS) without any model using the same grid resolution as that of LES ($48 \times 64 \times 48$).

Figure 2 shows the profile of streamwise velocity versus y/δ. The DNS data (Piomelli and Liu, 1995) (replotted for negative angular velocity) are represented by circle symbols, the LES data are represented by a solid line, and the coarse grid DNS data are represented by a dashed line. Good agreement has been found between the LES and DNS data. It is interesting that the U velocity distribution is no longer symmetric about the center line. The maximum U velocity is shifted from the centerline toward the stabilized wall due to the Coriolis force. The coarse and fine grid DNS data are almost indentical.

Figures 3, 4, and 5 show the rms distributions (normalized by the average value of u_τ on two walls) for velocity fluctuations in x, y, and z directions, respectively. The rms fluctuations are enhanced near the unstable side (y = 1.0) but reduced near the stable side of the channel (y = −1.0). It is noticeable that the profile of v_{rms} becomes a one-peak distribution instead of the two-peak distribution obtained without rotation. This is also

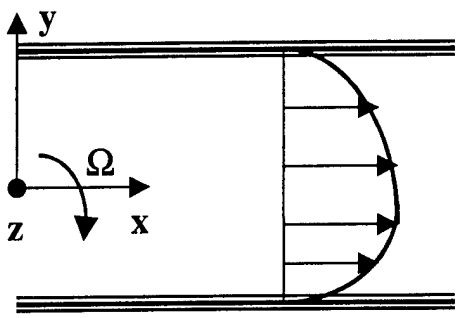

Fig. 1 Coordinate system for rotating channel flow

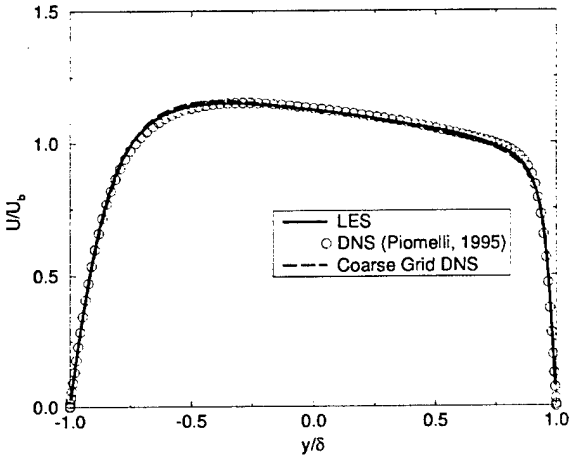

Fig. 2 Streamwise velocity distribution, isothermal channel flow

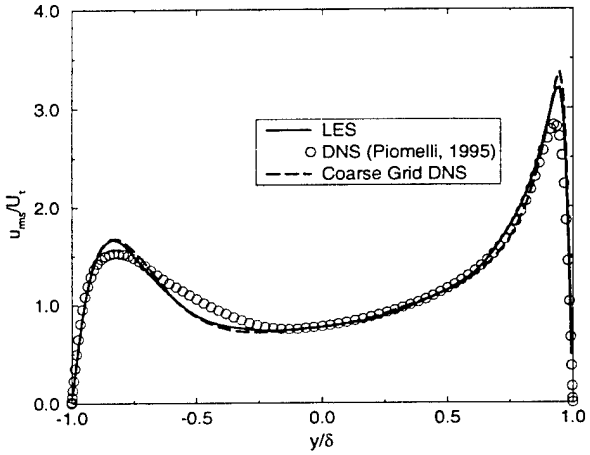

Fig. 3 Streamwise velocity rms distribution, isothermal flow

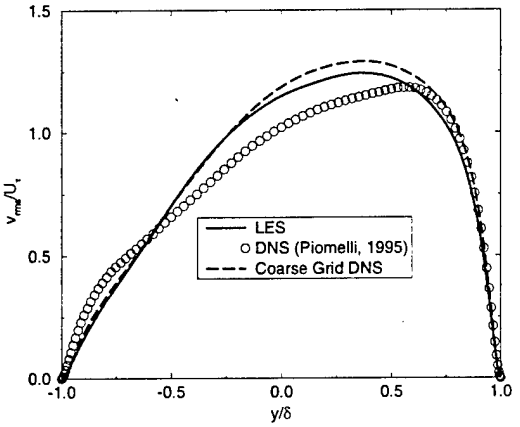

Fig. 4 Normal velocity rms distribution, isothermal flow

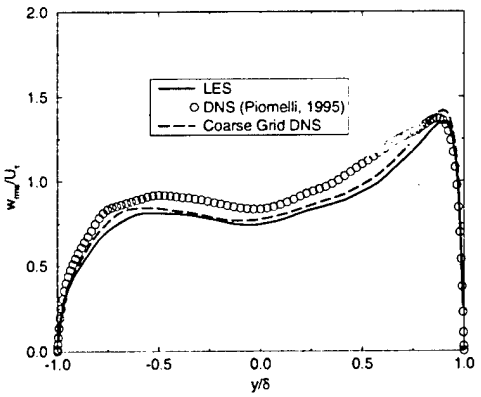

Fig. 5 Spanwise velocity rms distribution, isothermal flow

due to the fact that the Coriolis force acts in the y direction. These results agree reasonably well with those of Piomelli's, validating the current LES formulation. The coarse grid DNS data, in general, slightly overestimate velocity fluctuations compared

with the LES data. There is an overshoot for the coarse grid DNS in the prediction of velocity fluctuations near the upper (top) wall. The reason might be that the current grid resolution is not fine enough for DNS.

Figure 6 shows the streamwise velocity profiles for the high heating (HH), high cooling (HC) and low heating (LH) cases. The influence of rotation is reflected in the asymmetric distribution of velocities for all three cases. The U velocity profile for HC is above that of LH, but the profile for HH is below that of LH. This is, in part, because in the figures the streamwise velocity has been normalized by the average of u_τ at the two walls and u_τ is significantly influenced by property variations in the flow. Previous researchers (Huang et al., 1995; Dailey, 1997; Dailey and Pletcher, 1998) have proposed a semi-local definition of friction velocity, in which the local density is used instead of the wall density.

$$u_\tau^* = \sqrt{\frac{\tau_w}{\rho(y)}}$$

When u_τ^* is used to replace u_τ, the resulting semi-local distribution, seen in Fig. 7 shows that the three profiles collapsed toward the low heating curve.

The mean temperature profiles are plotted in global coordinates in Fig. 8. The friction temperature parameters T_τ is defined below,

$$T_\tau = \frac{q_w}{\rho_w c_p u_\tau} \tag{15}$$

As was observed for the velocity profiles, the high heating and high cooling temperature profiles nondimensionalized by wall values depart from the low heating results.

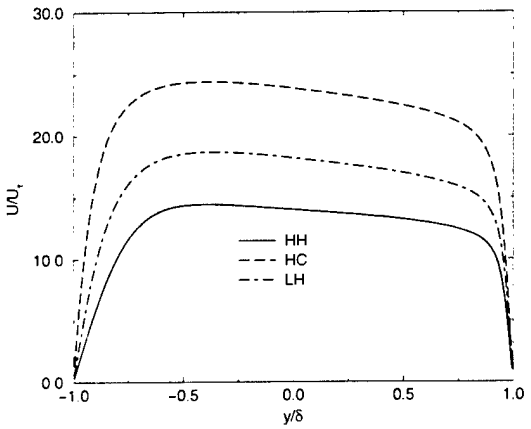

Fig. 6 Profile of u velocity

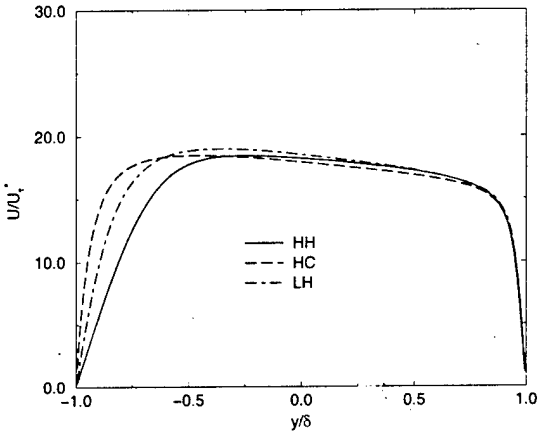

Fig. 7 Profile of semilocal u velocity.

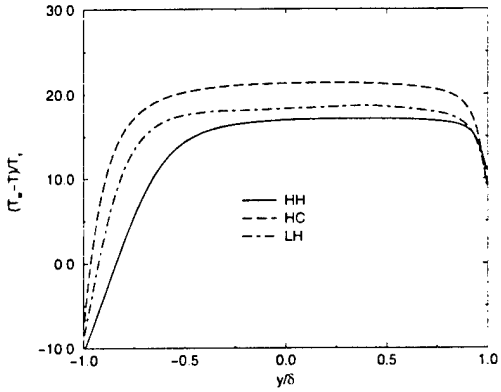

Fig. 8 Temperature profiles

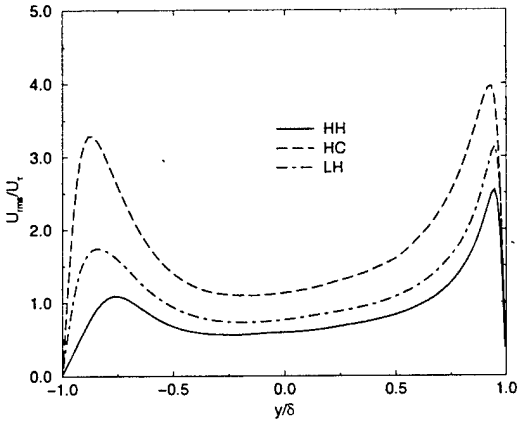

Fig. 9 Distribution of u_{rms}

The root-mean-square of the velocity fluctuations with respect to Reynolds ensemble averages are plotted in global coordinates in Figs. 9 and 10. Again, larger velocity fluctuations were found near the unstable side as a consequence of rotation, and the high heating and cooling values varied significantly from the low heating result. As before, the values are normalized by the average of u_τ for the two walls.

Figures 11, 12, and 13 show the viscous, resolved, and modeled SGS shear stress distributions normalized by the average of the two wall shear stresses. The results indicate that rotation increased the shear stress near the unstable side but suppressed the shear stress near the stable side.

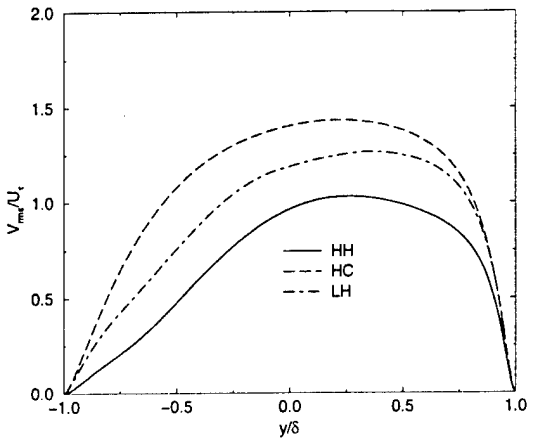

Fig. 10 Distribution of v_{rms}

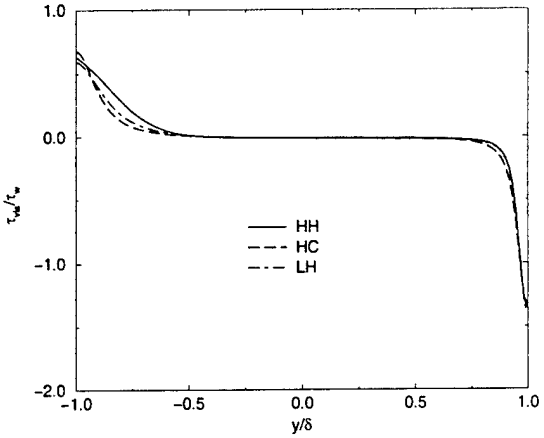

Fig. 11 Distribution of viscous stress

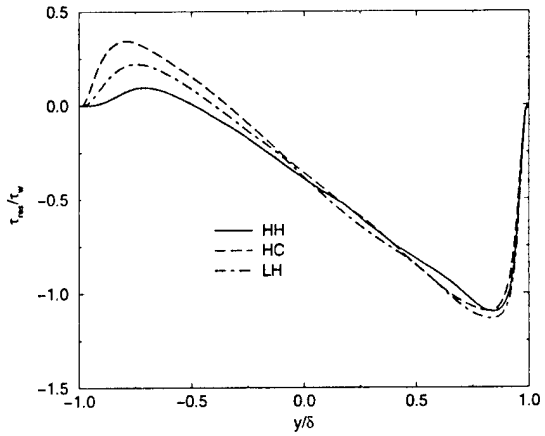

Fig. 12 Distribution of resolved stress

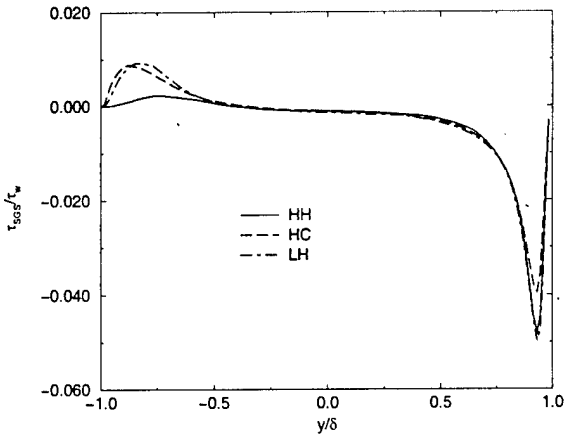

Fig. 13 Distribution of SGS stress

It can be observed that the shear stress on the unstabilized wall is approximately twice as large as on the stabilized wall and that the resolved turbulent stress follows a similar trend.

Figures 14, 15, and 16 show the heat conduction, resolved turbulent heat flux and modeled SGS heat flux distributions normalized by the wall heat flux. The same trends can be observed as for the shear stress distributions, suggesting that heat transfer was increased near the unstable side but decreased near the stable side because of rotation.

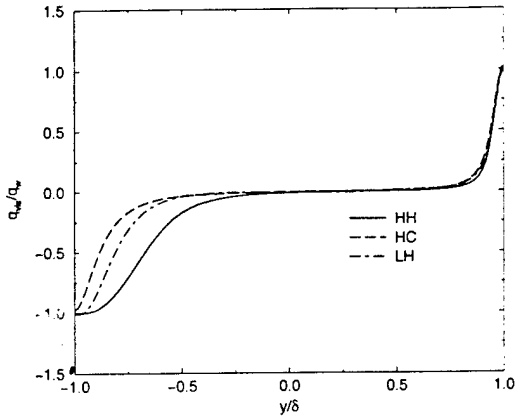

Fig. 14 Distribution of molecular heat conduction

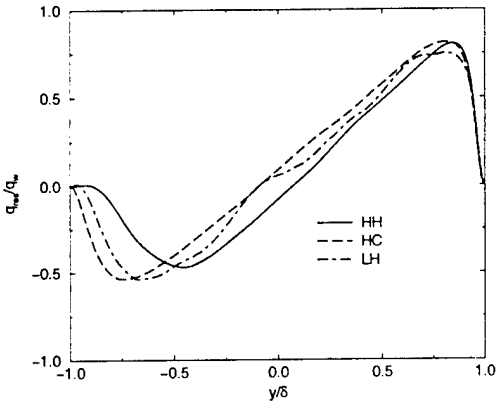

Fig. 15 Distribution of resolved heat flux

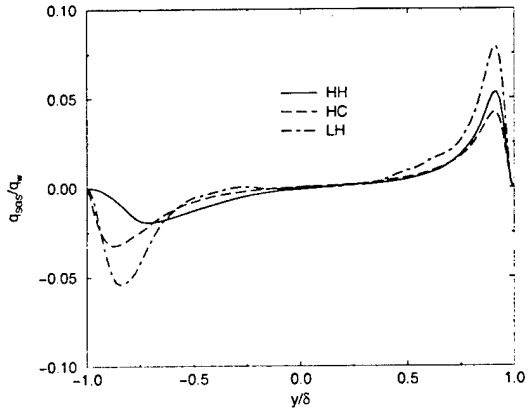

Fig. 16 Distribution of SGS heat flux

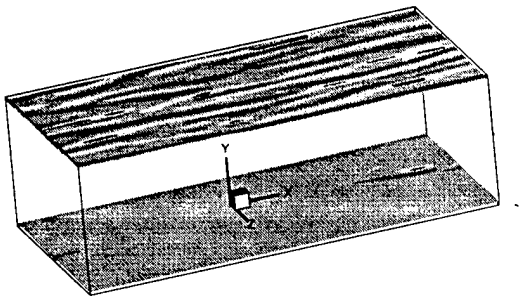

Fig. 17 Contours of wall normal vorticity, high heating

Figure 17 shows the wall normal instantaneous y-component of vorticity at planes located at $y/\delta = \pm 0.99$ for the HH case. Near the trailing (top) wall small scale turbulent structures are evident but few can be seen near the leading wall. Similar results were observed for all the rotation cases considered although the magnitudes of the vorticity was generally smaller for the low heating case.

Friction and heat transfer parameters are given in Table 1. The tabulated $\Delta T = T_{w,top} - T_{w,bot}$ is the temperature difference across the channel and T_b is the bulk temperature. The Nusselt numbers are based on the wall heat flux, channel hydraulic

Table 1. Summary of Wall Parameters, Rotating Flow

Case	$u_{\tau,top}$	$u_{\tau,bot}$	$\frac{\Delta T}{T_b}$	Nu_{top}	Nu_{bot}	$C_{f,top}$	$C_{f,bot}$
Low Heating	0.0696	0.0468	–0.0321	64.27	19.36	0.00557	0.00238
High Heating	0.0889	0.0801	–0.8038	83.04	15.38	0.00617	0.00288
High Cooling	0.0760	0.0384	0.3645	51.81	19.73	0.00519	0.00248

diameter, the bulk thermal conductivity, and the difference between the wall and bulk temperatures. The friction coefficient is defined as

$$C_f = \frac{\tau_w}{\frac{1}{2}\rho_b U_b^2}$$

The ratio of friction velocity at the top wall to that at the bottom wall is approximately 1.8, 1.5, and 1.1 for high cooling, low heating, and high heating, respectively. The low heating case had a relative temperature difference of 3.2%, but high heating and high cooling cases exhibited much larger temperature differences, namely, 80% and 34%, respectively. The Nusselt number at the top wall was found to be 2-5 times larger than on the lower wall, whereas the friction coefficients at the top wall were about twice as large as those at the bottom wall. Such a large increase in Nusselt number due to rotation for the heating case was not expected and the cause is currently under investigation. Density is a factor in the Coriolis force and significant density variations across the flow may well be responsible for the sensitivity of the Nusselt number to heating level.

5.0 CONCLUSIONS

The LES results (mean velocity and velocity fluctuations) agreed well with Piomelli's DNS data for the incompressible isothermal rotating channel flow at a rotation number of 0.144. Turbulent channel flow with low heating and with heating and cooling rates of magnitudes large enough to cause significant variation in the temperature-dependent fluid properties were simulated. All simulations were performed under the influence of spanwise system rotation. The distribution of mean velocity and mean temperature were influenced by system rotation, creating asymmetric profiles. The shift of peak values was toward the stable side of the channel. This shift would likely be altered in ducts of finite aspect ratios where mean secondary flows would influence the distributions. In general, the system rotation was found to suppress turbulent velocity fluctuations and shear stresses near the stable side of the channel, but enhance them near the unstable side. Accordingly, turbulent temperature fluctuations and turbulent heat flux are decreased near the stable side of the channel, but increased near the unstable side of the channel. The streamwise and spanwise *rms* velocity fluctuations were seen to differ by about a factor of two near the two walls. The ratio of wall shear stress and heat flux on the two sides ranged between a factor of 2 and 3. The ratio of Nusselt numbers at the two walls was as large as a factor of 5 as can be seen from Table 1. Using semi-local wall coordinates for velocity and temperature distributions tended to collapse curves of high heating and high cooling into that of low heating. It is interesting, too, that the distribution of v_{rms} is changed significantly (from a two-peak profile to a one-peak profile) due to the Coriolis force acting in the y direction.

6.0 PUBLICATIONS

The following dissertation describes research that has been supported in part by this grant:

Meng, N., 2000. "Large eddy simulation of turbulent flows with property variations, rotation and complex geometry," Ph.D. dissertation, Iowa State University.

Conference proceedings that describe research that has been supported in part by this grant include:

Meng, N. and Pletcher, R. H., 2000. "Large eddy simulation of rotating channel flows with and without heat transfer," Proceedings of the ASME Heat Transfer Division-2000, Vol. 5, pp.213-224.

Meng, N. and Pletcher, R. H., 2001. "Large eddy simulation for a rib-roughened turbulent channel flow with heat transfer and property variations," to be presented at the Third AFOSR International Conference on DNS/LES, August, 2001.

7.0 PERSONNEL

Professor R. H. Pletcher served as the principal investigator throughout the duration of this grant. Steve Sass and Ning Meng participated as graduate student research assistants.

8.0 REFERENCES

Dailey, L.D. and Pletcher, R.H., 1996. "Evaluation of multigrid acceleration for preconditioned time-accurate navier-stokes algorithms," *Computers and Fluids*, Vol. 25, pp. 791-811.

Dailey, L.D., 1997. "Large eddy simulation of turbulent flows with variable property heat transfer using a compressible finite volume formulation," Ph.D. dissertation, Iowa State University.

Dailey, L.D. and Pletcher, R.H., 1998. "Large eddy simulation of constant heat flux turbulent channel flow with property variations," 36th AIAA Aerospace Sciences Meeting and Exhibit, January 12-15, 1998, Reno, NV.

Han, J.C., Zhang, Y.M., and Lee, C.P., 1994. "Influence of surface heating condition on local heat transfer in a rotating square channel with smooth walls and radial outward flow," *Journal of Turbomachinery*, Vol. 116(1), pp. 149-158.

Hopfinger, E.J., 1989. "Turbulence and vortices in rotating fluids," *Theoretical and Applied Mechanics*, pp. 117-138, Elsevier.

Huang, P.G., Coleman, G.N., and Bradshaw, P., 1995. "Compressible turbulent channel flow - a close look using DNS data," AIAA paper, 95-0584.

Johnston, J.P., Halleen, H.M., and Lezius, D.K., 1972. "Effects of spanwise rotation on the struture of two-dimensional fully developed turbulent channel flow," *Journal of Fluid Mechanics,* Vol. 56, pp. 533.

Kristoffersen, R. and Andersson, I.H., 1993. "Direct simulations of low-reynolds-number turbulent flow in a rotating channel," *Journal of Fluid Mechanics*, Vol. 256, pp. 163-197.

Meng, N., Pletcher, R.H., and Simons, T.A., 1999a. "Large eddy simulation of a turbulent channel flow with a rib-roughened wall," AIAA 99-0423, 37th AIAA Aerospace Sciences Meeting and Exhibit, January 11-14, 1999/Reno, NV.

Meng, N., Pletcher, R.H., and Dailey, L.D., 1999b. "Compressible large eddy simulation for turbulent channel flow with constant heat flux", AIAA 99-3356, 14th AIAA Computational Fluid Dynamics Conference, June 29-July 2, 1999, Norfolk,VA.

Meng, N. and Pletcher, R. H., 2000. "Large eddy simulation of rotating channel flows with and without heat transfer," Proceedings of the ASME Heat Transfer Division-2000, Vol. 5, pp.213-224.

Moin, P., Squires, K., Cabot, W., and Lee, S., 1991. "A dynamic subgrid-scale model for compressible turbulence and scalar transport," *Physics of Fluids A*, Vol. 3, pp. 2746-2757.

Nicoud, F., 1998. "Numerical study of a channel flow with variable properties," Annual Research Briefs (1998), Center for Turbulent Research, pp. 289-310.

Piomelli, U. and Liu, J.H., 1995. "Large-eddy simulation of rotating channel flows using a localized dynamic model," *Physics of Fluids*, Vol. 7(4), pp. 839-848.

Tafti, D.K., and Vanka, S.P., 1991. "A numerical study of the effects for spanwise rotation on turbulent channel flow," *Physics of Fluids A*, Vol. 3, pp. 642.

Tritton, D.J., 1978. "Turbulence in rotating fluids," *Rotating Fluids in geophysics*, pp. 105-138, Academic Press.

Tritton, D.J., 1985. "Experiments on turbulence in geophysical fluid dynamics," *Turbulence and Predictability in Geophysical Fluid Dynamics and Climate Dynamics*, pp. 172-192, North-Holland.

Wang, W.P. and Pletcher, R.H., 1995. "Evaluation of some coupled algorithms for large eddy simulation of turbulent flow using a dynamic sgs model," AIAA paper 95-2244.

Wang, W.P. and Pletcher, R.H., 1996. "On the large eddy simulation of a turbulent channel flow with significant heat transfer," *Physics of Fluids*, Vol. 8, pp. 3354-3366.